Structural phase transitions of tellurium nanoplates under pressure*

Li Chao(李 超)[a], Arfan Bukhtiar[b], Shen Xi(沈 希)[a], Kong Pan-Pan(孔盼盼)[a], Wang Wei-Peng(王伟鹏)[a], Zhao Hao-Fei(赵豪飞)[a], Yao Yuan(姚 湲)[a], Zou Bing-Suo(邹炳锁)[b], Li Yan-Chun(李延春)[c], Li Xiao-Dong(李晓东)[c], Liu Jing(刘 景)[c], Jin Chang-Qing(靳常青)[a], and Yu Ri-Cheng(禹日成)[a]†

[a] *Beijing National Laboratory for Condensed Matter Physics, Institute of Physics, Chinese Academy of Sciences, Beijing* 100190, *China*
[b] *Beijing Key Laboratory of Nanophotonics and Ultrafine Optoelectronic Systems, Beijing Institute of Technology, Beijing* 100081, *China*
[c] *Institute of High Energy Physics, Chinese Academy of Sciences, Beijing* 100039, *China*

(Received 5 October 2014; revised manuscript received 10 December 2014; published online 19 January 2015)

In situ high-pressure angle dispersive x-ray diffraction experiments using synchrotron radiation on Te nanoplates were carried out with a diamond anvil cell at room temperature. The results show that Te-I with a trigonal structure transforms to triclinic Te-II at about 4.9 GPa, Te-II transforms to monoclinic Te-III at about 8.0 GPa, Te-III turns to rhombohedral Te-IV at about 23.8 GPa, and Te-IV changes to body centered cubic Te-V at 27.6 GPa. The bulk moduli B_0 of Te nanoplates are higher than those of Te bulk materials.

Keywords: tellurium nanoplates, phase transition, high pressure

PACS: 64.70.Nd, 61.05.cf, 64.60.–i **DOI:** 10.1088/1674-1056/24/3/036401

1. Introduction

The high-pressure (HP) behavior of the group VI element tellurium (Te) has been investigated for a long time.[1–6] At ambient conditions, Te is a semiconductor. It has a trigonal (Te-I) crystal structure with highly anisotropic characteristics consisting of helical chains along the *c* axis. The three atoms in the unit cell are linked by covalent-like bonds to the nearest neighbors along the chain and via van der Waals interactions to the second neighbors lying along adjacent chains.[7] Te has a series of complicated phase transitions under high pressure. It should be noted that the structural behavior within the pressure range of 4–29 GPa has remained controversial so far.[1–6] In the past, a generally accepted phase transition sequence was that trigonal Te-I changes to monoclinic Te-II at about 4 GPa, monoclinic Te-II turns to orthorhombic Te-III at about 7 GPa, orthorhombic Te-III transforms to rhombohedral Te-IV at about 11 GPa, and rhombohedral Te-IV changes to body centered cubic (bcc) Te-V at about 27 GPa.[1–3] However, these results have been suspected by a diffraction study of Te-III and Te-IV.[4] In Ref. [4], it was suggested that Te-III exists in the pressure range of 7–27 GPa and the structure of Te-III is monoclinic, which is different from the previous result.[2] Later, x-ray diffraction (XRD) showed a rather different HP scenario as follows. Trigonal Te-I partially transforms to triclinic Te-II at 4 GPa, and Te-I and Te-II coexist from 4 GPa to 4.5 GPa. Then, incommensurately modulated (IM) monoclinic Te-III appears at 4.5 GPa. Te-II and Te-III coexist from 4.5 GPa to 8 GPa, and Te-II disappears at 8 GPa while Te-III exists until 29 GPa. Finally, Te-III transforms into the bcc Te-V above 29 GPa.[5,6]

It should also be noted that studies on the phase transition behaviors of Te under pressure have only been focused on Te bulk or power so far. During the past few decades, semiconductor nanomaterials (such as wires, rods, belts, tubes, spheres, plates, and flowers) have attracted significant interest for their excellent properties on future electronic, photonic and life-science applications. As a typical semiconductor, Te-I has a narrow direct band gap (band gap energy 0.35 eV) at ambient conditions. It exhibits many unique properties such as photoconductivity, catalytic activity, piezoelectricity, thermoelectricity, and nonlinear optical responses,[8–11] which make it a multifunctional material in many electric and optoelectronic devices, such as self-developing holographic recording devices, radiative cooling devices, gas sensors, field-effect devices, and infrared acousto-optic deflectors.[10,12,13] Besides, the controlled growth of multi-morphology Te crystals (such as one-dimensional nanorods and nanowires, and two-dimensional hierarchical flowerlike microarchitecture)[11,14–19] has developed maturely, which makes it possible to be used in nanodevices. Generally, the nanomaterials have many promising physical properties in strength, thermal, electronic, and magnetic aspects in contrast with the conventional bulk materials. Especially, their surface features and energy band structures exhibit remarkable differences. So the structural transition of nanomaterials under pressure has become a hot point. How-

*Project supported by the State Key Development Program for Basic Research of China (Grant No. 2012CB932302) and the National Natural Science Foundation of China (Grant Nos. 10974235 and 11174336).

†Corresponding author. E-mail: rcyu@aphy.iphy.ac.cn

© 2015 Chinese Physical Society and IOP Publishing Ltd

ever, the transition behaviors of Te nanomaterials under pressure have rarely been investigated so far.[20] A study focuses on the relationship between the phase transition pressure and grain size. It is found that the phase transition pressures are higher for the smaller nanocrystals (NCs).[20] In Ref. [20], the Te NCs were compressed up to 20 GPa which is low to observe the whole process of the phase transition. Considering the importance of determining the structural transition behaviors of Te nanomaterials under pressure, the structures were reexamined until about 29.6 GPa in this paper. We report the structural stability of Te nanoplate using the *in situ* high-pressure angle dispersive x-ray diffraction (ADXD) technique.

2. Experiments

The Te nanoplates are the by-products of the CdTe nanocrystals. The thiol-capped CdTe nanocrystals were obtained using a chemical approach with hydrazine hydrate in an aqueous solution of $Cd(NO_3)_2$, mercaptoethylamine and tellurium. In an alkaline aqueous solution, hydrazine hydrate reduced commercial Te to be an active reactant, which was further reduced to negative bivalent telluride for the preparation of CdTe nanocrystals. If Ethylenediamine Tetramethylenephosphonic acid is added into the solution at the boiling point (the pH value decreases in solution) and the solution is kept at the temperature for 2 h, CdTe nanocrystals decompose and suspension occurs. After centrifuge, the Te nanoplates are obtained. The thickness of the nanoplates is tens of nanometers and the width is 500–800 nm, which depend on the reaction time.

The ADXD experiment on Te nanoplates under external pressure from 0 to about 29.6 GPa at room temperature was performed at the Beijing Synchrotron Radiation Facility (BSRF). The x-ray wavelength was 0.6199 Å and the beam size was 35×15 μm^2 in diameter. High pressure was generated by using a symmetric type DAC with 300 μm culets. The sample was loaded into the sample chamber in a T301 stainless steel gasket, and the pressure was calibrated by using the ruby luminescence technique. The diffracted x-rays were recorded with a MAR345 image plate detector placed at a distance of about 349.35 mm, which was calibrated by CeO_2. The FIT2D program was used to display and integrate the diffraction rings on the image plate. No pressure transmitting medium was used in our experiments.

3. Results and discussion

At ambient conditions, Te bulk materials crystallize in a trigonal structure with a space group of $P3_121$. For Te nanoplates, they possess the same structure as the Te bulk materials at ambient conditions. Figure 1 shows the high-pressure *in situ* ADXD patterns of Te nanoplates up to about 29.6 GPa. With increasing pressure, all the diffraction peaks shift to a higher scattering angle, which indicates a gradual reduction of the unit cell volume. There are four phase transitions during loading pressure (Figs. 1(a)–1(c)). The first phase transition of Te nanoplates occurs at about 4.9 GPa, indicated by the appearance of diffraction peaks positioned at about 12°, 12.3°, 12.6°, 14.3°, and 14.6° (marked by the upward arrows) and by the decrease of the original peaks (marked by the downward arrows) in Fig. 1(c). The first phase transition pressure (4.9 GPa) of the Te nanoplates is similar to that of Te powder (4.5 GPa).[5] Above 4.9 GPa, trigonal Te-I changes to Te-II, nevertheless the structure of Te-II has still been disputed so far. In the past, it was reported as a monoclinic structure with 4 atoms per unit cell and a structure comprising puckered layers through alternating long and short bonds, which contains zigzag chains.[1] Recently, the structure of Te-II was reexamined by Hejny *et al.*[5] It was found that Te-II has a triclinic structure, whose superspace group is $I\bar{1}$. We use these two different structures of Te-II to assign out the diffraction peaks, respectively. The results show that the diffraction peaks in Fig. 1(c) can be assigned more reasonably by using the structure given by Ref. [5]. Therefore, it is suggested that Te-II has a triclinic structure with a superspace group of $I\bar{1}$. In our experiment, no pressure transmitting medium was used, which makes the Te nanoplates be compressed under a non-hydrostatic environment. This may cause the coexistence of Te-I and Te-II in the pressure arrange of 4.9–6.2 GPa.

The second phase transition of Te nanoplates starts from at about 8.0 GPa, characterized by the decrease of the peak positioned at about 15° (Fig. 1(c)). On further compression, the three diffraction peaks at about 12° and the two diffraction peaks at about 15° are merged, which are all marked by the downward arrows as shown in Fig. 1(b). It should be noted that the structure of Te-III is still controversial up to now. It was previously accepted as an orthorhombic phase,[2] but this conclusion was disturbed by a subsequent diffraction study of Te-III and Te-IV up to 33 GPa,[4] which suggested that Te-III is a monoclinic structure. After that, the high pressure experiment of Te suggested that Te-III has an incommensurate monoclinic structure with superspace group $I'2/m(0q0)s0$.[5] According to the relevant report,[5] many of the Te-II reflection peaks could be interpreted as the splitting of Te-III reflection peaks. This interpretation is coincident with our results. The diffraction peaks at 15.1 GPa in our experiment can be assigned by the structure of monoclinic Te-III, whose superspace group is $I'2/m$. It was reported that the phase transition pressures in Te nanocrystals (NCs) goes higher for smaller ones. The two phase transitions pressures are 7.2 GPa and 10.3 GPa, 5.9 GPa and 8.8 GPa, and 4.0 GPa and 6.8 GPa,[20] respectively, for 20 nm Te NCs, 90 nm Te NCs, and bulk Te. The Te nanoplates used in our ADXD experiment is tens of nanome-

ters thick and 500–800 nm in width, which is larger than the NCs used in Ref. [20], and show phase transitions at 4.9 GPa and 8.0 GPa which are lower compared to the NCs but higher than that of bulk Te, consistent with the results of Ref. [20].

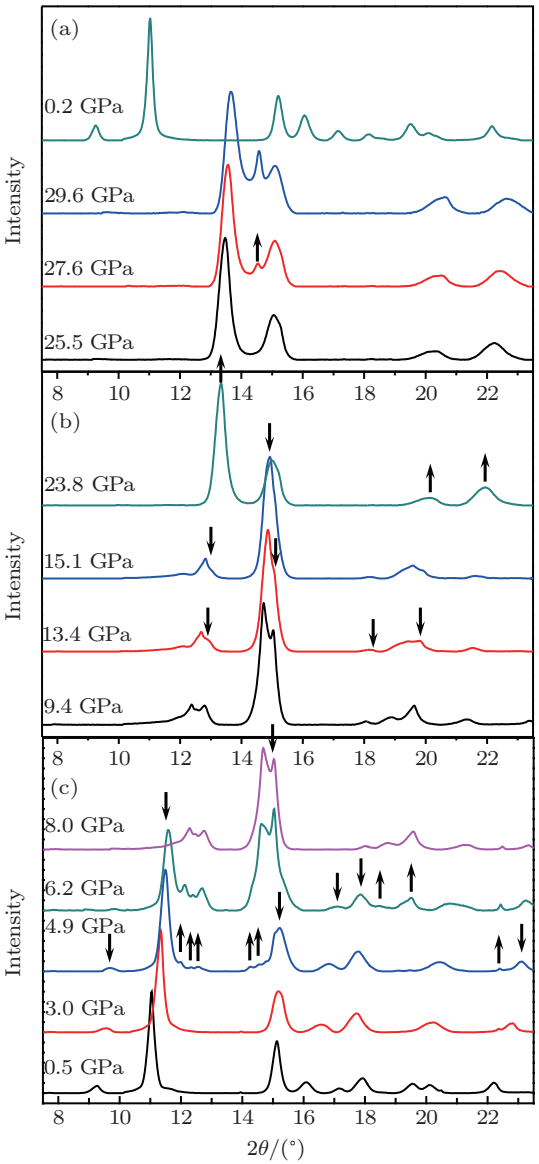


Fig. 1. (color online) ADXD patterns of the Te nanoplates at different pressures. (a) The phase transition from Te-I to Te-II and from Te-II to Te-III. (b) The phase transition from Te-III to Te-IV. (c) The phase transition from Te-IV to Te-V.

The phase transition from Te-III to Te-IV was characterized by the disappearance of some original diffraction peaks (marked by the downward arrows) and the appearance of new peaks (marked by the upward arrows) at 23.8 GPa as shown in Fig. 1(b). According to the relevant studies,[2,3] these new peaks can be assigned to (001), $(01\bar{1})$, $(11\bar{1})$, and (011) reflections of rhombohedral structure with space group $R\bar{3}m$. The transition pressure (23.8 GPa) of the Te nanoplates from Te-III to Te-IV is slightly lower than that of Te powder (27 GPa reported in Ref. [4] and 29.2 GPa reported in Ref. [5]). The main reason for this distinction may be the different high pressure experiment conditions. The high pressure experiments both in Refs. [4] and [5] used a pressure transmitting medium, so their experiment conditions are much closer to hydrostatic pressure. In our high pressure experiment, no pressure transmitting medium was used, which makes the Te nanoplates be compressed under a non-hydrostatic environment. Under the non-hydrostatic condition, there is a pressure gradient in the chamber, thus the shear stress which effects on the Te nanoplates is larger than that under hydrostatic condition. This shear stress can induce the slip between crystal planes, which could give rise to the phase transition at a lower pressure.

The fourth phase transition of Te nanoplates happens at about 27.6 GPa, indicated by the appearance of diffraction peaks positioned at about 14.5° (marked by the upward arrows in Fig. 1(a)). This means that the Te nanoplates transform from a rhombohedral structure to a bcc structure (Te-V).

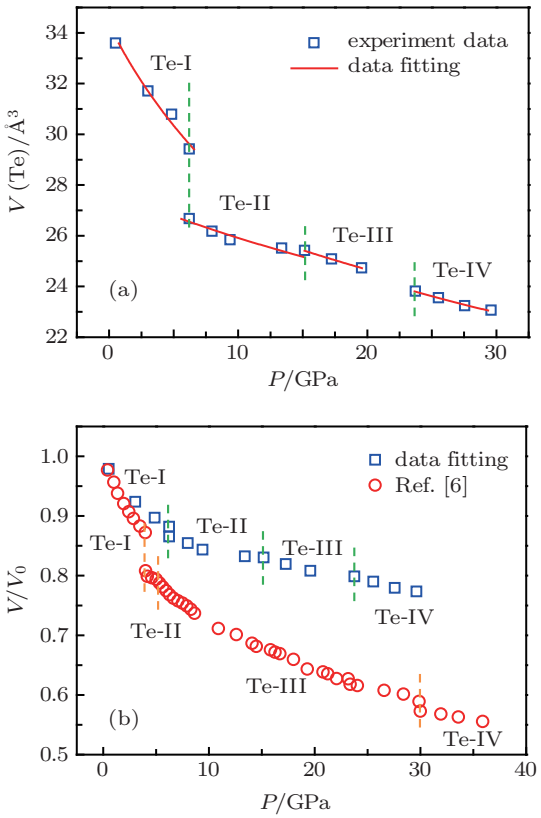


Fig. 2. (color online) (a) The volume change of Te nanoplates and (b) the compressibility of Te nanoplates up to 29.6 GPa.

The volume of one Te atom under different pressures can be well derived from the refined lattice parameters and the pressure–temperature–volume dependence can be decided systematically by an appropriate equation of state. The Birch–Murnaghan (BM) equation[21,22] of the third order is valid for the isotropic case in a quasi-hydrostatic pressure environment. It is described as

$$P = \frac{3}{2}B_0\left[\left(\frac{V}{V_0}\right)^{-7/3} - \left(\frac{V}{V_0}\right)^{-5/3}\right] \times \left\{1 - \frac{3}{4}\left(4 - B_0'\right)\left[\left(\frac{V}{V_0}\right)^{-2/3} - 1\right]\right\}, \quad (1)$$

where V and V_0 represent the volumes of one Te atom at pressure P and ambient pressure, respectively, while B_0 and B_0' are the isothermal bulk modulus and its first-order pressure derivative, respectively. The volume of Te nanoplates as a function of pressure is shown in Fig. 2(a). The red lines are the fitting results fitted by the BM equation. From these fittings, the values for the bulk modulus B_0 are obtained, which are shown in Table 1. The bulk modulus B_0 of Te nanoplates is 30.6 GPa at ambient conditions, which is larger than that of bulk or powder Te (23 GPa).[23,24] For Te nanoplates, the volume exhibits a monotonous decrease with increasing pressure during the whole process of phase transitions. There is an intense reduction of the volume of Te powder at 6.2 GPa accompanied by the phase transition from Te-I to Te-II, which indicates a first order phase transformation.

Table 1. The bulk modulus B_0 and zero-pressure volume V_0 obtained from the BM equation.

Phase	B_0/GPa	Standard error/GPa	V_0/Å^3	Standard error/Å^3	B_0'
Te-I	30.6	5.5	34.3	0.6	4
Te-II	123.6	19.8	30.2	0.3	4
Te-III	110.5	18.7	30.6	0.4	4
Te-IV	81.6	11.9	28.9	0.6	4

The relative volume change V/V_0 of Te nanoplates as a function of pressure is shown in Fig. 2(b). The volume change behavior of Te powder under pressure cited from Ref. [6] is also plotted in Fig. 2(b) for comparison. The volume change of Te nanoplates is smaller than that of Te powder under the same pressure, as shown in Fig. 2(b), which indicates that the Te nanoplates are more difficult to compress due to the size effect than Te powder under the same compression conditions. It should be noted that the B_0 is getting smaller for Te-III and Te-IV. At the moment, we do not know the reason for this, but a similar phenomenon was also reported by other groups in Ho_2O_3 and Dy_2O_3 compounds.[25,26]

4. Conclusions

An *in situ* high-pressure ADXD experiment for Te nanoplates was performed at room temperature. The results show that Te-I with a trigonal structure transforms to triclinic Te-II at $\sim$ 4.9 GPa, Te-II transforms to monoclinic Te-III at $\sim$ 8.0 GPa, Te-III turns to rhombohedral Te-IV at $\sim$ 23.8 GPa, and Te-IV changes to bcc Te-V at 27.6 GPa. By fitting the relative volume versus pressure, it is shown that the bulk modulus B_0 of Te nanoplates is higher than that of Te bulk materials.

References

[1] Aoki K, Shimomura O and Minomura S 1980 *J. Phys. Soc. Jpn.* **48** 551
[2] Parthasarathy G and Holzapfel W B 1988 *Phys. Rev. B* **37** 8499
[3] Jamieson J C and McWhan D B 1965 *J. Chem. Phys.* **43** 1149
[4] Takumi M, Masamitsu T and Nagata K 2002 *J. Phys.: Condens. Mater.* **14** 10609
[5] Hejny C and McMahon M I 2003 *Phys. Rev. Lett.* **91** 215502
[6] Hejny C and McMahon M I 2004 *Phys. Rev. B* **70** 184109
[7] Marini C, Chermisi D, Lavagnini M, Castro D D, Petrillo C, Degiorgi L, Scandolo S and Postorino P 2012 *Phys. Rev. B* **86** 064103
[8] Song J M, Lin Y Z, Zhan Y J, Tian Y C, Liu G and Yu S H 2008 *Cryst. Growth Des.* **8** 1902
[9] Beauvais J, Lessard R A, Galarneau P and Knystautas E 1990 *J. Appl. Phys. Lett.* **57** 1354
[10] She G W, Shi W S, Zhang X H, Wong T L, Cai Y and Wang N 2009 *Cryst. Growth Des.* **9** 663
[11] Gautam U K and Rao C N R 2004 *J. Mater. Chem.* **14** 2530
[12] Engelhard T, Jones E D, Viney I, Mastai Y and Hodes G 2000 *Thin Solid Films* **370** 101
[13] Souilhac D, Billerey D and Gundjian A 1990 *Appl. Opt.* **29** 1798
[14] Liu Z P, Li S, Yang Y, Hu Z K, Peng S, Liang J B and Qian Y T 2003 *New J. Chem.* **27** 1748
[15] Mayers B and Xia Y N 2002 *J. Mater. Chem.* **12** 1875
[16] Mayers B and Xia Y N 2002 *Adv. Mater.* **14** 279
[17] Zhu H T, Zhang H, Liang J K, Rao G H, Li J B, Liu G Y, Du Z M, Fan H M and Luo J 2011 *Phys. Chem. C* **115** 6375
[18] Wang S, Guan W P, Ma D K, Chen X, Wan L, Huang S M and Wang J C 2010 *Cryst. Eng. Commun.* **12** 166
[19] Wang S, Zhang K J, Zhou H A, Guan W P, Ma D K, Lin J J, Zhang L J, Huang S M and Wang J C 2010 *Cryst. Eng. Commun.* **12** 3852
[20] Deng Z T, Bao Z X, Cao L, Chen D, Tang F Q, Wang F F, Liu C X, Zou B S and Muscat A J 2008 *Nanotechnology* **19** 045707
[21] Murnaghan F D 1944 *Proc. Nati. Acad. Sci. USA* **30** 244
[22] Perdew J P, Burke K and Ernzerhof M 1996 *Phys. Rev. Lett.* **77** 3865
[23] McCann D R and Cartz L 1972 *J. Appl. Phys.* **43** 4473
[24] Lingelbach W, Stuke J, Weiser G and Trensch J 1972 *Phys. Rev. B* **5** 243
[25] Jiang S, Liu J, Li X D, Bai L G, Xiao W S, Zhang Y F, Lin C L, Li Y C and Tang L Y 2011 *Appl. Phys. Lett.* **110** 013526
[26] Jiang S, Liu J, Lin C L, Bai L G, Zhang Y F, Li X D, Li Y C, Tang L Y and Wang H 2013 *Solid State Commun.* **169** 37